

## La<sub>2</sub>Hf<sub>2</sub>O<sub>7</sub> crystal and local structure changes on the fluorite – pyrochlore phase transition

V V Popov<sup>1,2,3</sup>, A P Menushenkov<sup>1</sup>, A A Yastrebtsev<sup>1</sup> and Ya V Zubavichus<sup>2</sup>

<sup>1</sup> National Research Nuclear University MEPhI (Moscow Engineering Physics Institute), Kashirskoe sh. 31, 115409 Moscow, Russia

<sup>2</sup> NRC “Kurchatov Institute”, pl. Akademika Kurchatova 1, 123182 Moscow, Russia

E-mail: victorvpopov@mail.ru

**Abstract.** The process of La<sub>2</sub>Hf<sub>2</sub>O<sub>7</sub> ( $r_{\text{La}^{3+}}/r_{\text{Hf}^{4+}} = 1.63$ ) nanocrystals formation and evolution upon calcinations up to 1400 °C has been investigated by means of synchrotron radiation X-ray diffraction (XRD) and Raman spectroscopy. It has been shown that isothermal calcination at 800 °C/3h of the X-ray amorphous precursor firstly leads to the formation of oxide nanocrystalline powders with a defect fluorite structure. In the temperature range 900 – 1000 °C we observed the nucleation and growth of pyrochlore nanodomains inside a well crystalline fluorite matrix. The pyrochlore-type superstructural ordering of cations and anions appears at calcinations temperature higher than 1000 °C.

### 1. Introduction

The compounds and solid solutions formed in «Ln<sub>2</sub>O<sub>3</sub> - MO<sub>2</sub>» systems (Ln – lanthanides, M – titanium subgroup elements) has intensively investigated due to their important scientific interest (order-disorder phase transitions [1, 2]; geometrically frustrated magnets [3], etc.) and technological applications (thermal barrier coatings [4]; solid electrolytes in high temperature solid oxide fuel cells [5]; neutron absorbing materials [6]; nuclear waste storage materials [7], etc.). The application functionality of materials depends on the crystal and local structure of used materials. The structural phase transition from the order *Fd-3m* pyrochlore structure to the disorder *Fm-3m* defect fluorite structure involves the randomization of the oxygen ions among the 48*f*, 8*b*, and 8*a* sites, and the cations between the 16*c* and 16*d* sites [8].

Lanthanides hafnates are the less investigated in the Ln<sub>2</sub>M<sub>2</sub>O<sub>7</sub> family. During some years we actively investigated the specific features of the structure formation in “boundary” compounds Ln<sub>2</sub>Hf<sub>2</sub>O<sub>7</sub> (Ln = Sm – Dy) with the cation ratio  $r_{\text{Ln}^{3+}}/r_{\text{M}^{4+}} \sim 1.46$  [9–11]. The aim of the present work is to study the formation and evolution of crystal and local structures in La<sub>2</sub>Hf<sub>2</sub>O<sub>7</sub> ( $r_{\text{La}^{3+}}/r_{\text{Hf}^{4+}} = 1.63$ ), which has the most thermodynamically stable pyrochlore phase among Ln<sub>2</sub>Hf<sub>2</sub>O<sub>7</sub> group, upon isothermal calcination of an amorphous precursor. We simultaneously observed the processes of cation ordering using synchrotron radiation X-ray diffraction and anion ordering using Raman spectroscopy upon the “fluorite - pyrochlore” phase transition.

### 2. Experimental

<sup>3</sup> To whom any correspondence should be addressed.



The starting materials were  $\text{La}(\text{NO}_3)_3 \cdot 6\text{H}_2\text{O}$  (99.96% purity) and  $\text{HfOCl}_2 \cdot 8\text{H}_2\text{O}$  (99.7% purity). Precursor (mixed La-Hf hydroxide) was prepared by co-precipitation of metal salts solution with ammonia  $\text{NH}_3 \cdot \text{H}_2\text{O}$  (analytical grade) [12]. The  $\text{La}_2\text{Hf}_2\text{O}_7$  powders were prepared by calcination of precursor at 600–1400 °C for 3 h in air. A more detailed experimental procedure was described in Refs [9–11].

The thermal behaviour of the dried powders was studied from 100 to 1400 °C using thermogravimetric analysis and differential scanning calorimetry (TG/DSC, Netzsch STA 409 PC Luxx) with a heating rate of 10 K  $\text{min}^{-1}$  in an argon flow of 30 mL/min in corundum crucibles.

Crystal structure of  $\text{La}_2\text{Hf}_2\text{O}_7$  synthesized powders was studied by X-ray powder diffraction at “Structural Materials Science” beamline of the Kurchatov synchrotron radiation source. Measurements were carried out in the transmission mode at  $\lambda = 0.68886$  Å. The Rietveld full-profile analysis of X-ray diffraction patterns was performed with the Jana2006 software [13].

FT–Raman spectra were recorded at research analytical center JSC “VNIICHT” on the Nicolet iS50 FT–IR spectrometer (Thermo Scientific) equipped with iS50 Raman module with a laser excitation wavelength of 1064 nm. The spectra were measured in wave number range from 100 to 3700  $\text{cm}^{-1}$  and were averaged out of 256 scans with a time interval of 2 s and a resolution of 4  $\text{cm}^{-1}$ .

### 3. Results and discussion

The freshly washed precipitate of mixed La-Hf hydroxide was strongly hydrated (~ 95% water). The XRD study showed that both wet and dry powders were amorphous. However, XRD pattern indicated the presence of the first broad maximum which pointed to origin of the local order in the precursor structure.

According to TG-analysis, the dry precursor had formula  $\text{La}_2\text{O}_3 \cdot \text{HfO}_2 \cdot 10.7 \text{H}_2\text{O}$ . Significant parts of weight loss up to 300 °C (~ 50% of total) and above 950 °C (6% of total) indicate a high degree of hydration and strong retention of OH-groups in the crystal lattice of the synthesized samples.

It has been found that primary crystallization of precursor occurs between 700–800 °C/3 h. At 800 °C the powder appears to be nanocrystalline (coherent scattering length – CSL – 35 nm). Its XRD patterns show reflections corresponding to a fluorite structure ( $Fm-3m$ ) with a unit cell parameter ( $a$ ) of ~5.33 Å. A further increase in the calcination temperature leads to the narrowing of diffraction peaks (Figure 1a) owing to the increase of CSL values and the decrease in microstrain values ( $\epsilon$ ) (Table 1).

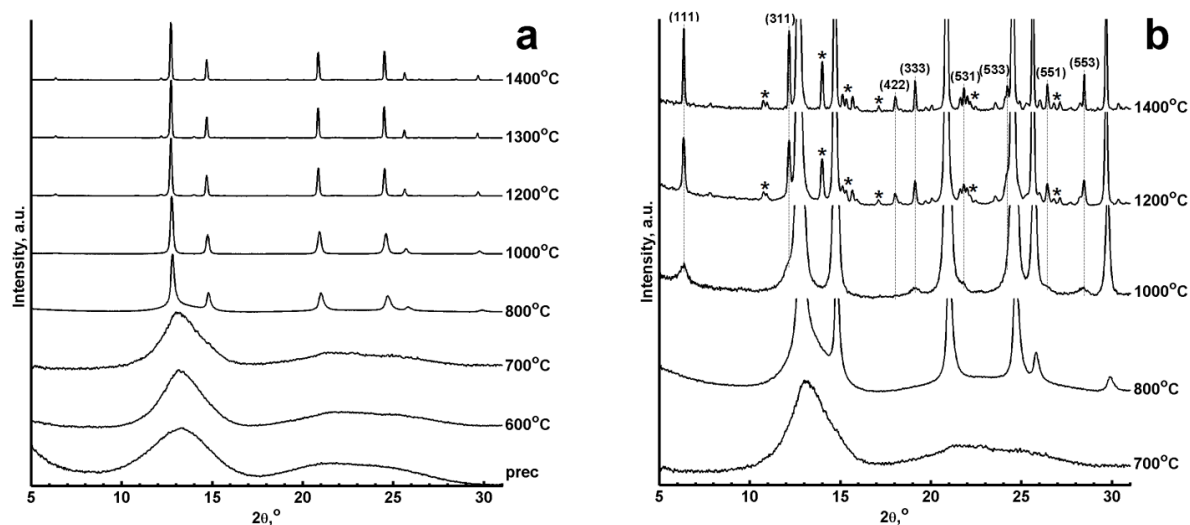


**Figure 1.** XRD patterns of  $\text{La}_2\text{Hf}_2\text{O}_7$  powders obtained by calcination of the precursor at different temperatures (shown on the corresponding curves) at 3 h in the air: (a) general pattern, (b) in a narrower range. In brackets are the reflection indices of the pyrochlore phase. \* - impurity of  $\text{HfO}_2$ .

The crystallization pattern for  $\text{La}_2\text{Hf}_2\text{O}_7$  starts qualitatively changing at temperature  $\sim 1000^\circ\text{C}$ . The XRD patterns of the powders synthesized at temperatures  $\geq 1000^\circ\text{C}/3\text{ h}$  show the appearance of superstructure peaks (111) (main), (311), (531) and others, which point to the onset of pyrochlore cationic ordering ( $Fd-3m$ ). From Figure 1b, it can be noted that the superstructure reflections remain significantly broader than the basic peak characteristic of fluorite. The XRD quantitative analysis (Table 1) enables to suggest that, in the case of  $\text{La}_2\text{Hf}_2\text{O}_7$  sample calcinations in temperature range  $900\text{--}1000^\circ\text{C}$ , the cationic ordering in the pyrochlore phase presumably occurs in separate regions (nanodomains) distributed over bulk crystals with the fluorite structure. It should be noted, that the observed “amorphous  $\rightarrow$  fluorite  $\rightarrow$  pyrochlore” phase transformation is consistent with Ostwald’s step rule. Similar results were obtained earlier for  $\text{Ln}_2\text{Hf}_2\text{O}_7$  ( $\text{Ln} = \text{Sm} - \text{Dy}$ ) [11] and  $\text{Gd}_2\text{Zr}_2\text{O}_7$  [14].

**Table 1.** Temperature dependence of atomic crystal structure parameters of  $\text{La}_2\text{Hf}_2\text{O}_7$  powders.

		Temperature, $^\circ\text{C}$				
		800	1000	1200	1300	1400
Crystal structure	Parameter					
$Fm-3m$	CSL, nm	35	115	149	445	839
	$\varepsilon$ , %	1.258	1.083	0.242	0.032	0.022
$Fd-3m$	CSL, nm	-	17	72	375	462
	$\varepsilon$ , %	-	0.317	0.386	0.743	0.610
$a$ , $\text{\AA}$		5.3328	10.7253	10.7531	10.7644	10.7546
% wt. $\text{HfO}_2$ (XRD / Raman)		-	2.4 / 1.2	4.1 / 4.4	4.8 / 5.1	6.2 / 6.1

The results of Raman spectroscopy investigations are presented in Figure 2. As shown in Figure 2, all the six pyrochlore modes  $E_g$  ( $321\text{ cm}^{-1}$ ),  $A_{1g}$  ( $499\text{ cm}^{-1}$ ) and  $4F_{2g}$  ( $304$  main,  $401$ ,  $520$  and  $755\text{ cm}^{-1}$ ) are observed in the Raman spectra of  $\text{La}_2\text{Hf}_2\text{O}_7$  powders prepared at temperature  $\geq 1000^\circ\text{C}$ . These results are in good agreement with [15].

Quantitative analysis of the obtained Raman spectra showed that the process of anion ordering of pyrochlore type in  $\text{La}_2\text{Hf}_2\text{O}_7$  powders begins at a lower temperature than the process of cation ordering (according to XRD data). However at calcinations temperature higher than  $1100^\circ\text{C}$  both the cation and anion sublattice of  $\text{La}_2\text{Hf}_2\text{O}_7$  became fully ordered. So above this temperature the “fluorite - pyrochlore” phase transformation is fully completed. As shown in Figure 3, the Raman spectra of  $\text{La}_2\text{Hf}_2\text{O}_7$  ( $1400^\circ\text{C}/3\text{h}$ ) clear indicate the presence of monoclinic  $\text{HfO}_2$  impurity. The  $\text{HfO}_2$  contents calculated from Raman spectra were in good agreement with XRD data (Table 1).

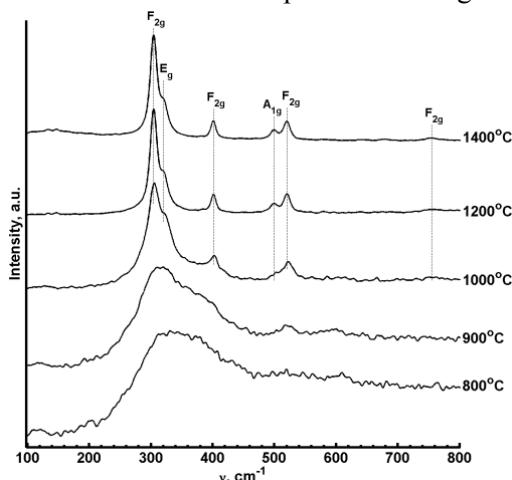


**Figure 2.** Raman spectra of  $\text{La}_2\text{Hf}_2\text{O}_7$  powders obtained by calcination of the precursor at different temperatures

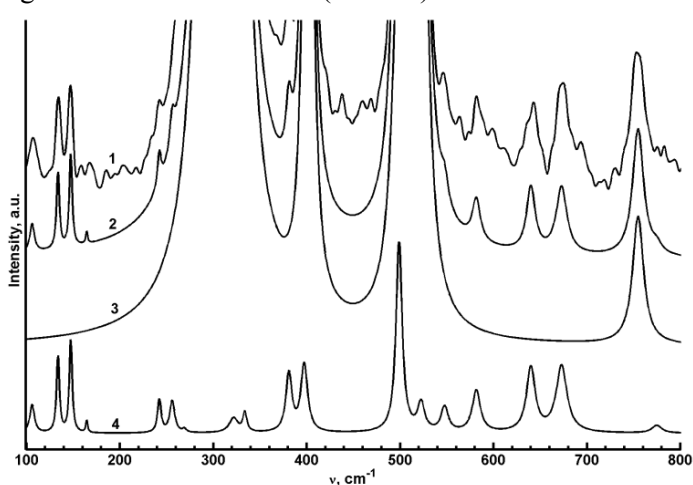


**Figure 3.** Raman spectra of powders  $\text{La}_2\text{Hf}_2\text{O}_7$  ( $1400^\circ\text{C}/3\text{ h}$ ) (1) and  $m\text{-HfO}_2$  phase (4); approximation curves: summary (2) and  $\text{La}_2\text{Hf}_2\text{O}_7$

(shown on the corresponding curves) (*Fd-3m*) (3).  
for 3 h in the air.

#### 4. Conclusion

The evolution of  $\text{La}_2\text{Hf}_2\text{O}_7$  crystalline and local structures upon calcination of initial mixed hydroxide has been studied simultaneously by using of synchrotron radiation XRD and Raman spectroscopy methods. It has been shown that isothermal calcination of the X-ray amorphous precursor at temperatures  $\geq 800$  °C first leads to the formation of oxide nanocrystalline powders with a defect fluorite structure and reveals an increase in coherent scattering lengths and a decrease in microstrain values upon calcination temperature increase. Heat treatment at temperature  $\geq 1000$  °C initiates nucleation and growth of nanodomains with pyrochlore-type superstructural ordering of cations and anions inside a microcrystalline fluorite matrix. At calcinations temperature higher than 1100 °C both the cation and anion sublattice of  $\text{La}_2\text{Hf}_2\text{O}_7$  became fully ordered and the “fluorite - pyrochlore” phase transformation is fully completed.

#### Acknowledgements

The authors thank N.A. Tsarenko (JSC “VNIChT”) for her help in Raman experiments and the Russian Science Foundation (grant 14-22-00098) for financial support.

#### References

- [1] Jiang C, Stank C R, Sickafus K E *et al* 2009 First-principles prediction of disordering tendencies in pyrochlore oxides *Phys. Rev. B* **79** 104203-1–104203-5
  - [2] Blanchard P E R, Liu S, Kennedy B J *et al* 2013 Investigating the local structure on lanthanoid hafnates  $\text{Ln}_2\text{Hf}_2\text{O}_7$  via diffraction and spectroscopy *J. Phys. Chem. C* **117** 2266-73
  - [3] Gardner J S, Gingras M J P, Greedan J E, 2010 Magnetic pyrochlore oxides *Rev. Modern Phys.* **82** 53–107
  - [4] Pan W, Phillpot S R, Wan C *et al* 2012 Low thermal conductivity oxides *MRS Bull.* **32** 917–22
  - [5] Yamamura H, Nishino H, Kakinuma K *et al* 2003 Electrical conductivity anomaly around fluorite–pyrochlore phase boundary *Solid State Ionics* **158** 359–65
  - [6] Risovany V D, Zakharov A V, Muraleva E M *et al* 2006 Dysprosium hafnate as absorbing material for control rods *J. Nucl. Mater.* **355** 163–70
  - [7] Ewing R C, Weber W J, Lian J 2004 Nuclear waste disposal - pyrochlore ( $\text{A}_2\text{B}_2\text{O}_7$ ): Nuclear waste form for the immobilization of plutonium and “minor” actinides *J. Appl. Phys.* **95** 5949–71.
  - [8] Nachimuthu P, Thevithasan S, Stutthanandan V *et al* 2005 Near-edge X-ray absorption fine-structure study of ion-beam-induced phase transformation in  $\text{Gd}_2(\text{Ti}_{1-y}\text{Zr}_y)_2\text{O}_7$  *J. Appl. Phys.* **97** 033518-1–033518-5
  - [9] Popov V V, Petrunin V F, Korovin S A *et al* 2011 Formation of nanocrystalline structures in the  $\text{Ln}_2\text{O}_3\text{-MO}_2$  systems ( $\text{Ln} = \text{Gd, Dy}$ ;  $\text{M} = \text{Zr, Hf}$ ) *Russ. J. Inorg. Chem.* **56** 1538–44
  - [10] Popov V V, Menushenkov A P, Zubavichus Ya V *et al* 2013 Characteristic features of the nanocrystalline structure formation in  $\text{Ln}_2\text{Hf}_2\text{O}_7$  ( $\text{Ln} = \text{Gd, Dy}$ ) compounds *Russ. J. Inorg. Chem.* **58** 1400–7
  - [11] Popov V V, Zubavichus Ya V, Menushenkov A P *et al* 2015 Lanthanide effect on the formation and evolution of nanocrystalline structures in  $\text{Ln}_2\text{Hf}_2\text{O}_7$  Compounds ( $\text{Ln} = \text{Sm–Dy}$ ) *Russ. J. Inorg. Chem.* **60** 16–22
  - [12] Popov V V 2015 Formation Regularities of Dispersed Hydrated Oxide Systems *Russ. J. Inorg. Chem.* **60** 420–7
  - [13] Petricek V, Dusek M and Palatinus L 2014 Crystallographic computing system JANA2006: General features *Z. Kristallogr.* **229** 345–52
- Popov V V, Zubavichus YaV, Menushenkov A P *et al* 2014 Short- and long-range order balance in

nanocrystalline  $\text{Gd}_2\text{Zr}_2\text{O}_7$  powders with a fluorite–pyrochlore structure  
*Russ. J. Inorg. Chem.* **59** 279–85

- [14] Kumar S, Gupta H C 2012 First principles study of dielectric and vibration properties of pyrochlore hafnates *Solid State Sci.* **14** 1405–11